Improving Tuning Range and Sensitivity of Localized SPR Sensors With Graphene

Ergun Simsek, *Senior Member, IEEE*

***Abstract*— This letter theoretically and numerically confirms that graphene can improve the tuning range and sensitivity of localized surface plasmon resonance (SPR) sensors. For an SPR sensor with metal nanoparticle arrays fabricated on top of a graphene-coated glass slide, the voltage applied to the graphene layer changes the graphene's optical conductivity and induced polarization of the nanoparticles. As a result of these modifications, the transmission and reflection characteristics of the device change. Numerical studies reveal that for the longitudinal mode, an increase of 2 eV in the chemical potential cause a 24-nm blue shift in the resonance wavelength with a sharper dip in the transmission spectrum and a 23% increase in the sensitivity.**

***Index Terms*— Graphene, optical sensors, surface plasmon resonance (SPR), tunable sensors.**

I. Introduction

FOR CHANGING testing environments like point-of-care diagnostics, it is advantageous to have sensors with tunable operating ranges. A set of sensors with different operating wavelengths can generate an extensive dataset for greater detection certainty despite any non-ideal environmental conditions. With its controllable optical conductivity and mechanically strong structure [1]–[6], graphene can be instrumental for such tunable sensors.

In a typical index-of-refraction sensing setup, the change in the reflected (or transmitted) light intensity due to the change in the flow channel is monitored [5]–[11]. Using a resonant structure might increase the contrast of the reflection (or transmission) spectra and make this monitoring easier. For example, if the resonant structure is a metal nanoparticle (MNP) array, then localized surface plasmon resonance (SPR) occurs when the interaction of sub-wavelength particles with incident light yield a collective oscillation of valence electrons at their maximum strength and a sharp dip (peak) at the transmission (reflection) spectra is observed near SPR wavelength. The material type, shape, dimensions, and periodicity of nanoparticles, as well as the incidence angle and background affect the resonance wavelength [5]–[11]. For example, Niu *et al.* demonstrate that SPR wavelength can be controlled by varying the thickness of the dielectric film between single layer graphene and metal nanoparticles [5], [6]. Apart from the unwanted deformations, most of these parameters cannot be modified after the fabrication. The resonance wavelength can be changed by changing the incidence angle, but this requires a meticulous alignment. Another way of designing a tunable sensor is by changing the optical properties of some components of the structure with applied voltage.

Manuscript received February 1, 2013; revised February 27, 2013; accepted March 14, 2013. Date of publication March 20, 2013; date of current version April 16, 2013.

The author is with the Department of Electrical and Computer Engineering, The George Washington University, Washington, DC 20052 USA (e-mail: simsek@gwu.edu).

Color versions of one or more of the figures in this letter are available online at http://ieeexplore.ieee.org.

Digital Object Identifier 10.1109/LPT.2013.2253316

II. Design

Assume an MNP array is fabricated on top of a graphene coated transparent substrate such as glass. In order to prevent direct contact between MNPs and graphene, a thin dielectric film can be placed between them, as shown in Fig. 1. On the two opposite sides of the structure, there are two long metallic contacts in order to make a connection between the graphene layer and a DC source. When the source is off, the device acts as a regular localized SPR based sensor with a resonance wavelength where the transmission (reflection) spectrum has a minimum (maximum). Turning on the DC source changes the optical properties of graphene and the induced dipole moment of each nanoparticle. Changing the potential distribution along the graphene layer results in a physical change in the inhomogeneous background and the charge distribution inside the nanoparticles, and hence the surface plasmon resonance of the whole structure. A precisely changed gate voltage should allow us to tune the sensor to any resonance wavelength within a reasonably wide range of wavelengths. The tuning range and sensitivity of such a sensor is examined as follows.

III. Numerical Analyses

The optical conductivity of graphene, written as $\sigma_c = \sigma_r + j\sigma_i$, can be calculated by following the formulation found in [4]. The formulation depends on angular frequency (ω), temperature (T), hopping parameter (t), and chemical potential (μ_c), which is a function of the carrier density and can be controlled by gate voltage, electric field, magnetic field, and/or chemical doping. Fig. 2 (a) and (b) show the real and imaginary parts of the conductivity, respectively, in the visible region as a function of chemical potential for $0 \text{ eV} < \mu_c < 4 \text{ eV}$. Fig. 2 (c) and (d) plot σ_r and σ_i for $\mu_c = 0$ eV (blue line) and $\mu_c = 2$ eV (red dashed line) only, which are the two special cases used below to demonstrate tuning capability. The results are obtained for $t = 2.7$ eV [12] at room temperature ($T = 300$ K). Fig. 2 indicates that when there is no bias voltage, graphene acts like a transparent conductor with an optical conductivity of $\sigma_c = \sigma_r$. When

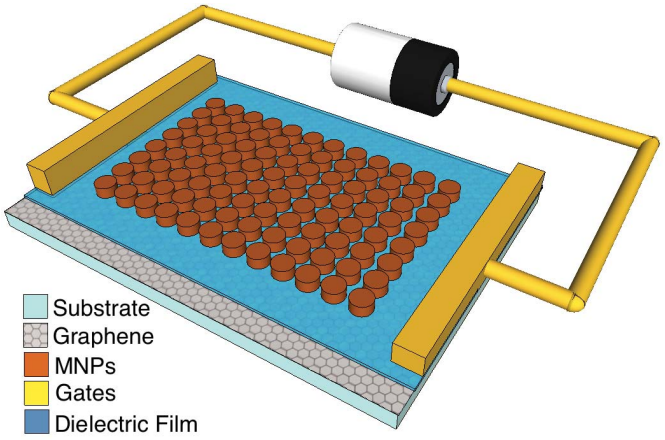

Fig. 1. MNP array fabricated on top of graphene-coated glass slide. For noncontact mode, there can be a thin dielectric layer between the graphene layer and MNPs. Voltage source is connected to via contacts at either end to the graphene layer. Dimensions are not proportional in the sketch.

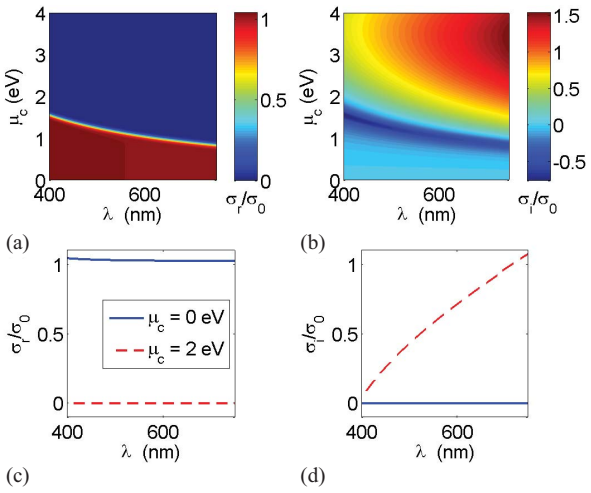

Fig. 2. Real (left) and imaginary (right) parts of the conductivity of graphene at room temperature in the visible region for (top) 0 eV $< \mu_c <$ 4 eV and (bottom) two different chemical potentials: $\mu_c = 0$ eV (blue solid line) and $\mu_c = 2$ eV (red dashed line). Results are normalized by σ_0, where $\sigma_0 = \pi e^2/2h$ and h is Planck constant.

voltage is applied, both real and imaginary parts of the optical conductivity start to change. As it is experimentally demonstrated in [3], increasing potential decreases σ_r and it experiences a dramatic drop when μ_c exceeds $\hbar\omega/2$. Conversely, the imaginary part has a minima at $\mu_c = \hbar\omega/2$ and it starts to increase as μ_c exceeds $\hbar\omega/2$ meaning that intraband absorption starts to dominate interband absorption.

In order to demonstrate tuning capability, the transmission spectrum is calculated using Wavenology EM (which is a general-purpose 3D electromagnetic wave simulation software), for a gold cylindrical nanoparticle array fabricated on top of a graphene coated glass slide under normal incidence with ($\mu_c = 2$ eV) and without a bias voltage ($\mu_c = 0$ eV). The radius and height of the cylindrical MNPs are 50 nm. Inter-particle spacing is 150 and 300 nm along the $\hat{x}$ and $\hat{y}$-axes, respectively. Periodic boundary conditions are applied at the $\pm x$ and $\pm y$ boundaries. Perfectly matched layers are

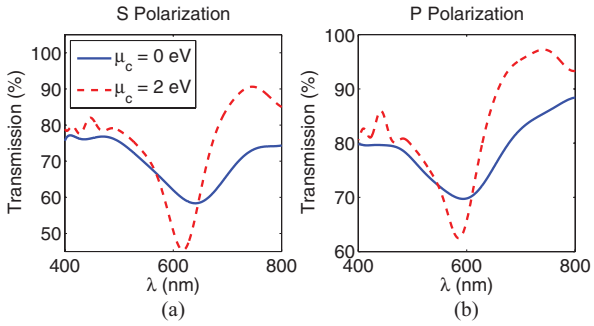

Fig. 3. Transmission versus wavelength of gold nanoparticle chain arrays under normal incidence. (a) S-polarization excites transverse modes. (b) P-polarization excites longitudinal mode.

applied at the $\pm z$ boundaries. For the optical constants of gold, the experimental values are used [13] rather than Drude model to eliminate any concern regarding the selection of appropriate values for plasmon and relaxation frequencies. The dielectric constant of glass is taken as 2.13. The thickness of the graphene layer is taken as 0.34 nm. A grid spacing of 0.17 nm is employed.

As shown in Fig. 3-(a), an increase of 2 eV in the chemical potential causes a 24 nm blue shift in the resonance frequency for the longitudinal mode ($\lambda_{\text{spr}} = 641$ nm and $\lambda_{\text{spr}} = 617$ nm for $\mu_c = 0$ eV and $\mu_c = 2$ eV cases, respectively). Even though the blue shift is much smaller (8 nm) for the transverse mode, see Fig. 3-(b), the transmission dip for both modes becomes narrower and sharper. As a result, unlike the broadening effect observed when the incidence angle is increased, increasing the gate voltage causes dips that are narrower and blue shifted, which facilitates monitoring.

The main mechanism behind this improvement can be understood more easily by converting the optical conductivity of graphene to a complex effective electrical permittivity as follows:

$$\epsilon_{\text{eff}} = 1 - j\frac{\sigma_c}{\omega\epsilon_0 d} = \left(1 + \frac{\sigma_i}{\omega\epsilon_0 d}\right) - j\frac{\sigma_r}{\omega\epsilon_0 d} \qquad (1)$$

where ω is the angular frequency and d is the thickness of graphene layer. It is evident from Eq. (1) that an increase in the imaginary part of the optical conductivity actually causes an increase in the real part of the permittivity, not in the imaginary part. As a result, increasing voltage indeed should cause a blue shifted and narrower transmission spectra.

Next, the potential of the sample structure for sensing is investigated by calculating the shift of the resonance wavelength as a function of the dielectric constant of the top medium, where MNPs reside. In order to verify improved sensitivity, the same numerical calculation method is followed for three different substrates: (a) bare glass slide, (b) graphene coated glass slide without bias voltage, i.e. $\mu_c = 0$ eV, and (c) graphene coated glass slide under bias voltage, i.e. $\mu_c = 2$ eV. Fig. 4 (a)–(c) shows transmission spectra for these three substrates assuming 5 different lossless dielectric media as the first layer with a refractive index of n, where $1 < n < 1.4$. In all three cases, a red shifted transmission spectra is observed due to an increasing refracting index of the top medium. The lossy nature of graphene causes a lower

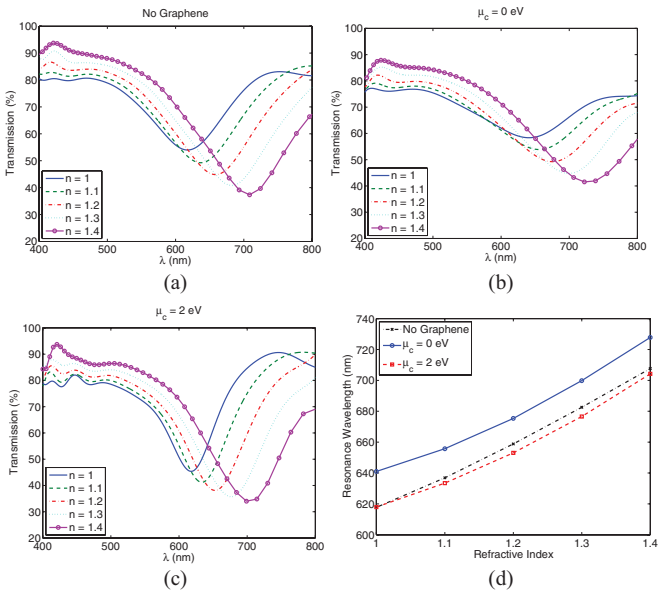

Fig. 4. Transmission versus wavelength for TE case normal incidence for gold MNPs fabricated. (a) Top of glass slide. (b) Top of graphene-coated glass slide for $\mu_c = 0$ eV. (c) Top of graphene-coated glass slide for $\mu_c = 2$ eV. Refractive index of first medium is linearly increased from 1 to 1.4. (d) Longitudinal mode SPR wavelength versus refractive index of medium where MNPs reside for three cases in (a)–(c).

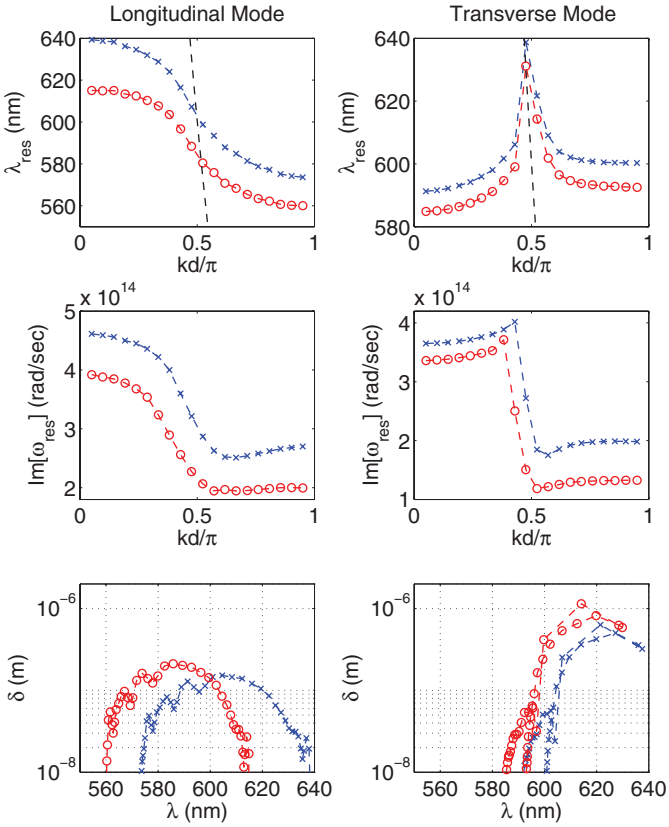

Fig. 5. Dispersion curves for longitudinal (left column) and first transverse (right column) excitation modes, respectively, for gold nanoparticles with height and radius of 50 nm, and center-to-center distances of 150 nm along the length of the chain. Bottom row: propagation lengths derived from dispersion curves for each mode. Blue dashed line with cross makers and red dashed line with red circles represent results obtained for $\mu_c = 0$ and $\mu_c = 2$ eV, respectively. Dashed black line depicts light line in air.

transmittance and broadened dips in (b) with respect to (a), but applied voltage suppress these negative effects.

Fig. 4(d) shows resonant wavelengths (where the transmission is minimum) as a function of the refractive index of the top medium. Even though the curves are not linear due to the dispersive nature of gold and graphene, it is still useful to define the sensitivity of the device in terms of relative change in resonance wavelength with respect to the change in the refractive index. Despite the fact that the MNP array on top of a bare glass slide has a higher sensitivity (225 nm per refractive-index unit (nm/RIU)) than the MNP array on top of a graphene coated glass slide at zero chemical potential (215 nm/RIU), increasing chemical potential to 2 eV with applied voltage improves sensitivity to 265 nm/RIU. As a result, it can be confidently said that graphene can indeed improve the tuning range and sensitivity of localized surface plasmon resonance sensors.

The dispersion relations are also obtained for the example design using layered medium coupled dipole approximation (LM-CDA), which is a fully-retarded theoretical model to analyze surface plasmon resonance properties of metal nanoparticle chains and arrays embedded in a multilayered medium [14]. LM-CDA assumes that nanoparticles act like oscillating dipoles when they are excited with incident light and surface plasmon resonance occurs when the dipole moment of a single oscillating dipole (nanoparticle) becomes equal to the induced dipole moment on that nanoparticle due to all other oscillating dipoles. LM-CDA puts this interaction into a matrix, and resonance frequencies can be calculated for which the matrix coupling the dipoles is singular. These frequencies are then mapped onto the dispersion relations. The main difference between LM-CDA and regular CDA based solvers [15] is the use of layered medium Green's functions [16] and the appropriate modification of particle polarizability [14]. Moreover, the Modified Long Wavelength Approximation (MLWA) is also employed [18] to account for the shift in plasmon frequency and polarizability due to the finite size of nanoparticles. The Fresnel reflection coefficients are modified for the graphene coated interfaces by following the formulation provided in [17].

Fig. 5 shows the dispersion curves for longitudinal (left column) and transverse (right column) excitation modes, respectively, for the gold nanoparticles with height and radius of 50 nm, and center-to-center distances of 150 nm along the length of the chain. Recall that MNPs reside on a graphene coated glass slide with a dielectric permittivity of 2.13. It is apparent that LM-CDA results perfectly agree with the numerical results shown in Figure 3-(a) and (b) for the normal incidence by yielding resonance wavelengths of 640 nm and 616 nm for the longitudinal mode and 592 and 585 nm for the transverse mode for $\mu_c = 0$ eV and $\mu_c = 2$ eV cases, respectively. Second, the tuning capability is observed. For example, by changing the applied voltage and angle of incidence for the longitudinal mode, we can tune the resonance wavelength of the sensor to any value between 575 nm and 640 nm. Moreover, this range can be even further increased by increasing the applied voltage. The second row of Fig. 5

shows the imaginary part of the complex radian frequency, which is an indicator of the loss experienced by the surface waves. In the last row, propagation lengths, which are derived from the dispersion curves for each mode, are depicted. For the transverse mode, approximately 1 μm of propagation length is possible, whereas it is only a couple hundred nm for the longitudinal mode. Since it is the sensing capability of the device that is of interest, not its wave-guiding efficiency, these extremely short propagation lengths are not crucial.

IV. Conclusion

In summary, the sensitivity and tuning range of localized surface plasmon resonance sensors can be increased with graphene. Numerical and theoretical results prove that the voltage applied to the graphene layer causes a blue shift in the transmission spectra of the plasmonic sensor. In addition to a narrower transmission dip, which facilitates monitoring, the overall sensitivity of the sensor is improved as well.

Acknowledgment

The author would like to thank the anonymous reviewers, Caroline Litchfield, and Arda Fuat for their constructive comments that greatly improve the manuscript. The author also thanks Wave Computation Technologies Inc. for providing 3D full wave simulation software and for generous technology support during the design process.

References

[1] K. S. Novoselov, *et al.*, "Two-dimensional gas of massless Dirac fermions in graphene," *Nature*, vol. 438, pp. 197–200, Sep. 2005.

[2] A. K. Geim and K. S. Novoselov, "The rise of graphene," *Nature Mater.*, vol. 6, no. 3, pp. 183–191, Mar. 2007.

[3] Z. Q. Li, *et al.*, "Dirac charge dynamics in graphene by infrared spectroscopy," *Nature Phys.*, vol. 4, no. 7, pp. 532–535, Jul. 2008.

[4] T. Stauber, N. M. R. Peres, and A. K. Geim, "Optical conductivity of graphene in the visible region of the spectrum," *Phys. Rev. B*, vol. 78, pp. 085432-1–085432-8, Aug. 2008.

[5] J. Niu, Y. Shin, Y. Lee, J. Ahn, and H. Yang, "Graphene induced tunability of the surface plasmon resonance," *Appl. Phys. Lett.*, vol. 100, no. 6, pp. 061116-1–061116-4, Feb. 2012.

[6] J. Niu, Y. Shin, J. Son, Y. Lee, J. Ahn, and H. Yang, "Shifting of surface plasmon resonance due to electromagnetic coupling between graphene and Au nanoparticles," *Opt. Express*, vol. 20, no. 18, pp. 19690–19696, Aug. 2012.

[7] J. Homola, "Present and future of surface plasmon resonance biosensors," *Anal. Bioanal. Chem.*, vol. 377, no. 3, pp. 528–539, Oct. 2003.

[8] H. K. Hunt and A. M. Armani, "Label-free biological and chemical sensors," *Nanoscale*, vol. 2, no. 9, pp. 1544–59, Jun. 2010.

[9] X. Fan, I. M. White, S. I. Shopova, H. Zhu, J. D. Suter, and Y. Sun, "Sensitive optical biosensors for unlabeled targets: A review," *Anal. Chim. Acta*, vol. 620, nos. 1–2, pp. 8–26, Jul. 2008.

[10] X. Fan and I. M. White, "Optofluidic microsystems for chemical and biological analysis," *Nature Photon.*, vol. 5, no. 10, pp. 591–597, Sep. 2011.

[11] K. B. Crozier, E. Togan, E. Simsek, and T. Yang, "Experimental measurement of the dispersion relations of the surface plasmon modes of metal nanoparticle chains," *Opt. Express*, vol. 15, pp. 17482–17493, Dec. 2007.

[12] R. R. Nair, *et al.*, "Fine structure constant defines visual transparency of graphene," *Science*, vol. 320, no. 5881, p. 1308, Jun. 2008.

[13] A. D. Rakic, A. B. Djurišic, J. M. Elazar, and M. L. Majewski, "Optical properties of metallic films for vertical-cavity optoelectronic devices," *Appl. Opt.*, vol. 37, pp. 5271–5283, Aug. 1998.

[14] E. Simsek, "Full analytical model for obtaining surface plasmon resonance modes of metal nanoparticle structures embedded in layered media," *Opt. Express*, vol. 18, no. 2, pp. 1722–1733, Jan. 2010.

[15] E. Simsek, "On the surface plasmon resonance modes of nanoparticle chains and arrays," *Plasmonics*, vol. 4, no. 3, pp. 223–230, Sep. 2009.

[16] E. Simsek, Q. H. Liu, and B. Wei, "Singularity subtraction for evaluation of Green's functions for multilayer media," *IEEE Trans. Microw. Theory Tech.*, vol. 54, no. 1, pp. 216–225, Jan. 2006.

[17] G. W. Hanson, "Dyadic Green's functions and guided surface waves for a surface conductivity model of graphene," *J. Appl. Phys.*, vol. 103, no. 6, pp. 064302-1–0643028, Mar. 2008.

[18] K. L. Kelly, E. Coronado, L. L. Zhao, and G. C. Schatz, "The optical properties of metal nanoparticles: The influence of the size, shape and dielectric environment," *J. Phys. Chem. B.*, vol. 107, no. 3, pp. 668–677, Mar. 2003.